

Growth, structural, optical, hardness and thermal studies of L-Arginine added TrisThiourea Zinc(II)Sulphate single crystals

K. KANAGASABAPATHY*, S. VETRIVEL^a, R. RAJASEKARAN^a

P.G. & Research Department of Physics, A.A. Government Arts College, Villupuram-605 602, India

^aP.G. & Research Department of Physics, Government Arts College, Tiruvannamalai-606 603, India

Tristhiourea Zinc(II)Sulphate(ZTS) and L-Arginine added Tristhiourea Zinc(II)Sulphate compounds were synthesized and single crystals were grown by slow evaporation technique. The cell parameters of the grown crystals were evaluated by single crystal X-ray diffraction technique. The powder X-ray diffraction patterns were recorded and indexed for further confirmation of crystalline nature of grown crystals. The crystalline perfection has been identified by etching studies. The presence of functional groups in the crystals has been confirmed by FTIR analysis. UV-Visible absorption spectra have been recorded to find the cutoff wavelength of the grown crystals. TGA/DTA and DSC studies show the thermal behavior of the grown crystals. The microhardness studies on the crystal samples revealed that the hardness increases with applied load for all the grown crystals. From the values of work hardening coefficient, it is found that ZTS and L-Arginine added ZTS crystals belong to the soft category materials. The second harmonic generation in the grown crystals was confirmed by Kurtz Perry powder method using Nd:YAG laser.

(Received June 10, 2012; accepted October 30, 2012)

Keywords: Growth from solution, X-ray diffraction, FTIR, Nonlinear material, Second Harmonic Generation

1. Introduction

In the past few decades, there has been remarkable interest in the growth and characterization of nonlinear optical material crystals. Hybrid NLO organic and inorganic complexes, semi-organic nonlinear optical (NLO) materials are capable of generating second harmonic frequency and play a vital role in the domain of optoelectronics [1-6]. In these materials, the high optical nonlinearity of pure organic compound is combined with the favorable mechanical and thermal properties of inorganic materials [7-11]. In the case of metal-organic coordination complexes, the organic ligand is usually more dominant in the NLO effect. Since metal compounds have high transparency in the UV region (because of their closed d^{10} shell), there has been focus on the group (II B) metals such as Zn, Cd, and Hg [12]. Thiourea molecule has large dipole moment [13] and has the ability to form extensive network of hydrogen bonds. The centrosymmetric thiourea molecule, when combined with inorganic salts yields non-centrosymmetric complexes which have enhanced non-linear optical properties. Metal complexes of thiourea include advantages of both organic and inorganic parts of the complex. Zinc(tris) Thiourea Sulphate (ZTS) is a promising semi-organic NLO material for second harmonic generation from metal complexes of thiourea [14-16]. ZTS possesses orthorhombic structure with space group $Pca2_1$ [17,18]. Most of the natural amino

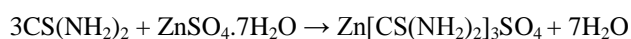
acids are individually exhibiting the NLO properties. Amino acids in solution at natural pH are predominantly zwitter ions rather than unionized molecules [6]. L-Arginine is an important polar amino acid, which shows higher SHG than other amino acids [7]. The amino group is protonated ($-NH_3^+$) and the carboxyl group is dissociated ($-COO^-$). In acidic solutions, amino acids have ionized the amino group ($-NH_3^+$) and carboxyl group is unionized. Most of the amino acids individually exhibit the NLO property due to donor amino group NH_3^+ acceptor carboxyl group COO^- and intermolecular charge transfer is also possible [17]. Therefore amino acids can be used as dopants and it was observed that there is enhancement in the material properties such as nonlinear optical and ferroelectric properties [2]. The effects of several dopants on structural and physical properties of metal complexes of thiourea and KDP have been reported [19,20]. Semi-organic nonlinear optical (NLO) crystals formed by amino acids with inorganic materials possess the advantages of high optical nonlinearity of the organic amino acids. It is reported that nonlinear performance can be improved by the addition of amino acid [21]. In the present investigation, ZTS has been added with optically active basic amino acid L-Arginine, in order to improve its SHG efficiency so that they can be used as better alternative to pure ZTS for optoelectronics applications. 1mole% of L-Arginine added ZTS crystals were grown by slow evaporation solution technique and the grown

crystals have been subjected to various characterization such as single crystal X-ray diffraction, powder X-ray diffraction, FTIR, UV-Visible spectroscopy, microhardness, thermal and etching studies. The Kurtz-Perry powder second harmonic generation (SHG) studies have been performed on the grown crystals.

2. Experimental

Synthesis and crystal growth

ZTS salt was synthesized by stoichiometric incorporation of Analar grade Thiourea (99% Merck) and zinc sulfate heptahydrate (99% Merck). The thiourea and zinc sulfate heptahydrate were taken in the ratio of 3:1 and were dissolved in deionised water of resistivity 18.2 MΩ.cm. The ZTS compound was prepared according to the following reaction,



The synthesized salt was purified by the repeated recrystallization process. A saturated aqueous solution was prepared and kept at room temperature for slow evaporation. Good quality single crystals with regular shape and size $13 \times 10 \times 6 \text{ mm}^3$ were grown within 20 days with approximate growth rate of 0.5 mm/day. For the growth of L-Arginine added ZTS crystals, 1mole% of L-Arginine [$\text{C}_6\text{H}_{14}\text{N}_4\text{O}_2$] was added to the solution of ZTS. Single crystals of size $14 \times 12 \times 7 \text{ mm}^3$ with good transparency were grown in 35-40 days. Figs. 1a and 1b shows the photographs of grown crystals.

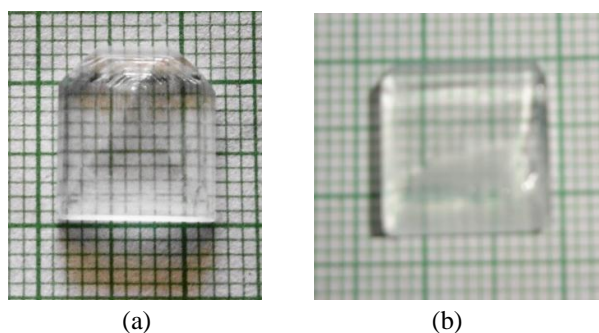


Fig. 1. Photographs of (a) ZTS and (b) L-Arginine added ZTS crystals.

3. Material characterization

The grown single crystals were subjected to single crystal X-ray diffraction (XRD) studies by employing a Kappa ApexII Nonius CAD4 diffractometer with MoK_α radiation ($\lambda = 0.71073 \text{ \AA}$). The powder XRD pattern of the grown crystal was recorded between 10°C and 80°C in steps of 2°C employing CuK_α radiation ($\lambda = 1.5406 \text{ \AA}$)

using Bruker Powder X-ray diffractometer. The optical absorption of the crystal was recorded using PerkinElmer Lambda 35 Model UV-Visible spectrophotometer in the wavelength region 200–900 nm. FTIR spectra of pure and amino acid added ZTS were recorded by Alpha Bruker spectrometer using KBr pellet technique in the wavelength range $4000\text{--}400 \text{ cm}^{-1}$. The nonlinear optical property in ZTS and L-Arginine added ZTS compound was confirmed by shining Nd:YAG laser of wavelength 1064 nm on thin plate of the grown crystals. The qualitative measurement of the second harmonic conversion efficiency was determined by Kurtz and Perry powder technique. In order to estimate the thermal behaviour, simultaneous thermo gravimetric analysis and differential thermal analysis of pure and L-Arginine added ZTS were carried out by using Universal 4.5A TA Instruments Q600 SDT simultaneous thermal analyzer in the temperature range: RT to 600°C (SiC furnace) and DSC measurement was carried out using TA Q20 Differential scanning calorimeter. The microhardness and etching studies were carried out on (1 0 0) plane of the grown crystals using Vicker's microhardness tester attached with an optical microscope (Micro-Duromet 4000E Hardness apparatus).

4. Results and discussion

4.1 Single crystal X-ray diffraction studies

Single crystal X-ray diffraction analysis of pure and 1mole% L-Arginine added ZTS crystals were carried out and their respective lattice parameter values are presented in Table 1.

Table 1. Lattice parameter values of the pure and L-Arginine added ZTS crystals.

| Crystal | a(Å) | b(Å) | c(Å) | V(Å ³) | $\alpha = \beta = \gamma$ |
|----------------------|-------|------|-------|--------------------|---------------------------|
| ZTS | 11.14 | 7.77 | 15.50 | 1341.65 | 90° |
| L-Arginine added ZTS | 11.15 | 7.79 | 15.48 | 1344.57 | 90° |

It is observed that ZTS and 1mole% of L-Arginine added ZTS grown crystals are belong to orthorhombic system with space group $\text{Pca}2_1$. These values are very close to the corresponding JCPDS (76-0778) values for pure ZTS [5]. In the L-Arginine added ZTS, there is slight increase in the unit cell volume compared to pure ZTS. The increase in volume may be due to the addition of L-Arginine in ZTS [6].

4.2 Powder X-ray diffraction studies

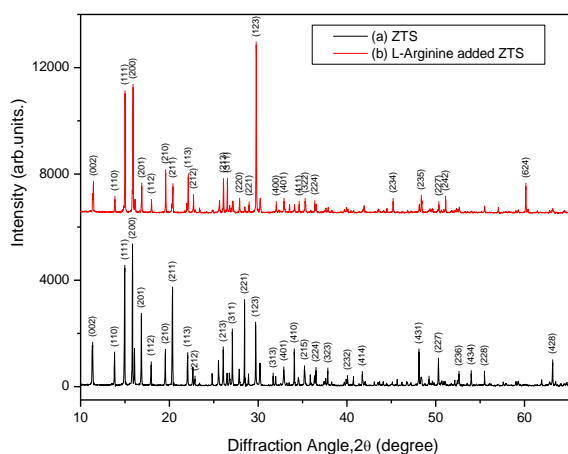


Fig. 2. Powder XRD patterns of (a) ZTS and (b) L-Arginine added ZTS crystals.

The Bragg's reflections in the powder XRD patterns (Fig. 2) were indexed for pure and doped ZTS crystals. The diffraction curve of ZTS shows a set of prominent peaks corresponding to (002), (111), (200), (211), (113), (221), (321), (401), (431), (227) and (428) planes. In the L-Arginine added ZTS, the peak intensities of reflections (113) and (123) have been increased due to doping, the peak intensities of reflections (201), (211) and (227) have been reduced. The peaks (323), (232), (434) and (428) in the doped crystal are disappeared and few new peaks (234), (242) and (624) are appeared. Comparing the powder XRD patterns, there is a small shift in the L-Arginine added XRD pattern of ZTS. This confirms the incorporation of L-Arginine in the ZTS crystal lattice. The observed lattice parameter values are in good agreement with the reported values [5]. The slight change in unit cell volume may be due to change in pH of the solution or due to the addition of amino acid [17].

4.3 FTIR studies

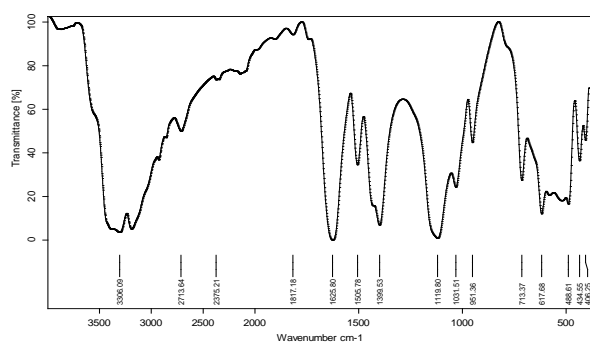


Fig. 3. FTIR spectrum of L-Arginine added ZTS crystal.

FTIR spectral analysis was carried out to identify the functional groups present in the synthesized compound (Fig. 3). In the ZTS complex, there are two possibilities by

which the coordination with metal can occur. It may be either through nitrogen or through sulfur. From the spectra, the N-H absorption bands in the high frequency region in thiourea are not shifted to lower frequencies on the formation of metal thiourea complex, thus coordination of thiourea occurs through sulfur in ZTS [15,16]. The NH, C=S and N-C-N stretching vibrations are also observed. The broad band lying in the range 2710–3377 cm^{-1} corresponds to symmetric and asymmetric vibrations of NH_2 group. The NH_2 bending vibration is observed at 1623 cm^{-1} [12]. The symmetric and asymmetric C=S stretching vibrations are observed in the bands 713 cm^{-1} and 1400 cm^{-1} . The absorption at 1502 cm^{-1} arising out due to N-C-N stretching vibration. The presence of sulphate ion is confirmed by the absorption band at 617 cm^{-1} and 1119 cm^{-1} [14,21]. Table 2 shows the comparison of assignments IR bands of 1mole% L-Arginine added ZTS with ZTS crystal. This shift in IR bands may be due to the addition of L-Arginine in ZTS.

Table 2. Assignment of FTIR band frequencies (cm^{-1}) of 1mole% L-Arginine added ZTS with pure ZTS.

| ZTS wavenumber cm^{-1} [21] | 1mole% L-Arginine added ZTS wavenumber cm^{-1} | Assignments |
|--------------------------------------|---|---------------------------------|
| 478.00 | 488.61 | $\delta_s(\text{S-C-N})$ |
| 619.04 | 617.68 | $\nu_{\text{as}}(\text{N-C-S})$ |
| 713.03 | 713.37 | $\nu_s(\text{C=S})$ |
| 1115.22 | 1119.80 | $\nu_s(\text{C-N})$ |
| 1400.39 | 1399.53 | $\nu_{\text{as}}(\text{C=S})$ |
| 1502.78 | 1505.78 | $\nu(\text{N-C-N})$ |
| 1626.09 | 1625.80 | $\delta(\text{NH}_2)$ |
| 3195.80 | - | $\nu_s(\text{NH}_2)$ |
| 3321.43 | 3306.09 | $\nu_{\text{as}}(\text{NH}_2)$ |

ν -stretching, δ -bending, s -symmetric, as -asymmetric.

4.4 UV-Visible spectral analysis

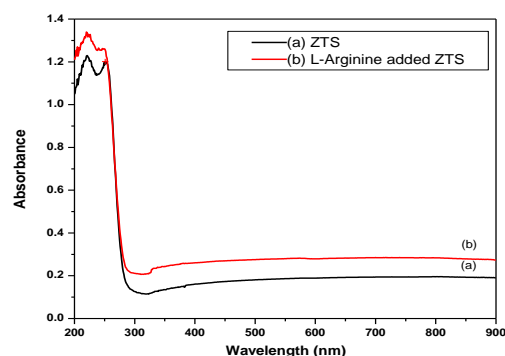


Fig. 4. UV-Visible absorption spectra of (a) ZTS and (b) L-Arginine added ZTS crystals.

For efficient NLO applications, the crystals should have lower cutoff between 200 and 400 nm. The optical absorption spectra were recorded using PerkinElmer Lambda 35 UV-Visible spectrophotometer in the wavelength region 200–900 nm with high resolution (Fig. 4). The absorption spectra show that both the grown crystals have lower cutoff wavelength (λ_{cut}) at around 268 nm. Near UV region, absorption arises from electronic transition associated within the thiourea units of ZTS. The orbital p-electron delocalization in thiourea arises from the mesomeric effect. This p-electron dislocation is responsible for its nonlinear optical response and absorption in near UV region [22]. Thus grown crystal has good transmission in UV as well as visible regions. It concludes that the adding of L-Arginine in ZTS is not affecting the cut-off wavelength and optical transmission property of ZTS [16,17,20]. The wide range of transparency in UV and the entire visible region shows that these crystals will be potential candidates for optoelectronic applications [23].

4.5 Thermal analysis

4.5.1 Thermo gravimetric analysis

The thermo gravimetric analysis (TGA) trace was carried out in the temperature range 25°–600 °C at a heating rate of 25 °C/min. The experiment was performed in nitrogen atmosphere. DTA curve of L-Arginine added ZTS shows that there are three endothermic transitions with the first one at 244.3 °C, the second at 296.6 °C and the third at 356.2 °C. The first endothermic peak coincides with the melting point of the crystal (244.3 °C). The melting point of pure ZTS is 249.47 °C [21]. When L-Arginine is added with ZTS, the melting point is decreasing slightly. TGA curve (Fig. 5a) shows that the sample undergoes a complete decomposition between 230 °C and 800 °C. The weight loss in the temperature range 231 °C – 280 °C is due to the liberation of volatile substances like sulphur oxide in the compound [14]. There is no major weight loss upto 236 °C. Thus, the crystal is thermally stable upto 236 °C ensuring its suitability of material for possible NLO applications. It is observed that there is maximum weight loss in the temperature range 236.90 °C – 348.47 °C compared with subsequent stages. A total weight loss of about 52.62 % occurred only at 325 °C. This shows the thermal stability of the crystal. A weight loss about 84.6% occurs at 590 °C. It concludes that the thermal stability of ZTS slightly decreasing with addition of amino acid L-Arginine. There is no phase transition till the material melts and this increase the temperature range for the use of crystal for NLO application. The absence of water in molecular structure is confirmed by the absence of weight loss around 100 °C. There is no decomposition upto melting point; this insures thermal stability of material for possible application in lasers.

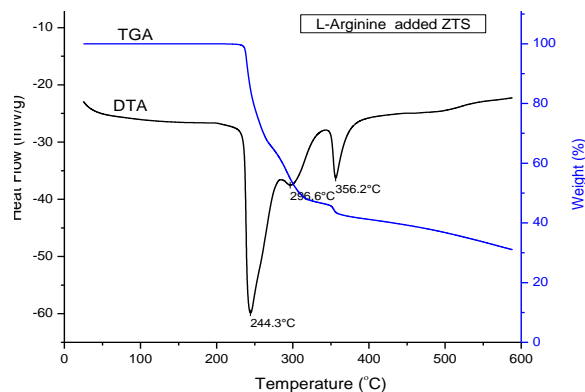


Fig. 5(a). TGA-DTA curve of L-Arginine added ZTS crystal.

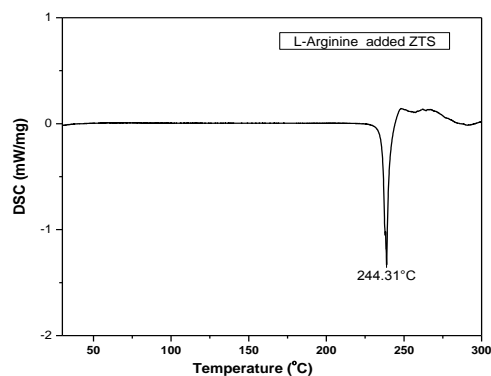


Fig. 5(b). DSC curve of L-Arginine added ZTS crystal

4.5.2 Differential scanning calorimetry studies

The differential scanning calorimetry (DSC) of grown pure ZTS and L-Arginine added ZTS crystals were carried out in nitrogen inert atmosphere between 0 and 600 °C. The DSC trace (Fig. 5b) shows exactly the same change shown by thermo gravimetric analysis. From the study of both thermo grams, it is clear that the melting point of grown crystals is 244.31 °C for L-Arginine added ZTS crystal.

4.6 Microhardness measurement

Hardness of a material is a measure of its resistance to plastic deformation. Indentations were made on (100) plane of pure and amino acid added ZTS crystals using Vicker's microhardness indenter for various loads with dwell time of 3s. For each load, several indentations were made and the average diagonal length (d) was measured to calculate the microhardness using the relation $H_v = 1.8544 P / d^2$ where H_v is the Vicker's hardness number, P is the applied load in kg and d is the diagonal length of the indented impression in mm and 1.8544 is a constant, a geometrical factor for the diamond pyramid.

It has been observed that the hardness value for pure ZTS crystal increases with applied load upto P=50 g due to work hardening of the surface layer [15,21]. Above 50 g, cracks were formed due to the release of internal stress

generated locally by indentation. The hardness value of L-Arginine added ZTS crystals is slightly higher than ZTS due to the dopant effect. A plot drawn between hardness number H_v and applied load P is shown in Fig. 6. The relation between the load and size of indentation is given by Meyer's law as $P = a d^n$ where P is load in kg, d is the diameter of recovered indentation in mm, a is constant and n is the work hardening coefficient. The plots between $\log P$ against $\log d$ for ZTS and L-Arginine added ZTS crystals are shown in the Fig. 7. The work hardening coefficient (n) for ZTS and L-Arginine added ZTS were found to be 5.74 and 3.63 respectively [14]. According to Onitsch [24], if n is greater than 1.6, the microhardness number increases with increase in load. Since the obtained values of n for the grown pure and L-Arginine added ZTS crystals are more than 1.6, the grown crystals belong to the soft category materials. The increase of hardness number with load will be useful for nonlinear optical applications.

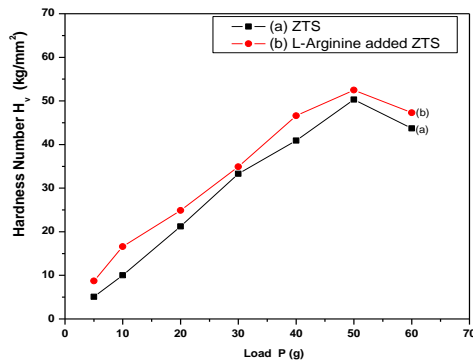


Fig. 6. Plot of Hardness number vs. applied load.

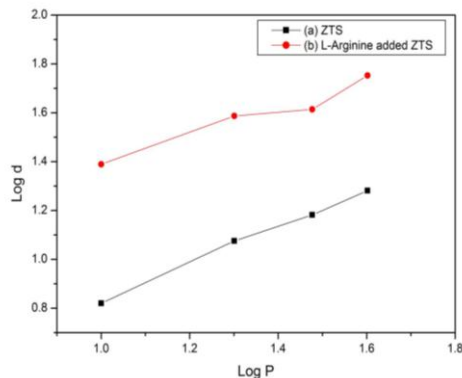
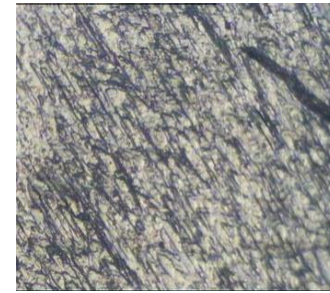


Fig. 7. Plot of $\log P$ against $\log d$.

4.7 Etching studies

Etching is a very simple and elegant technique to reveal the crystal defects and the crystal growth mechanism, which is able to develop some features such as growth striations, etch spirals, rectangular etch pits on the crystal surface. L-Arginine added ZTS crystal has been immersed for 10s, 30s and 60s in the water etchant and the samples were wiped out with dry filter paper. Using optical microscope in the reflection mode, the features of

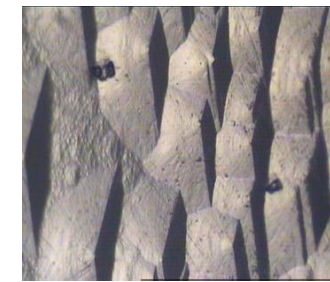
the crystal has been analyzed as shown in the Fig. 8. Some scattered etch pits and short striation were observed for the etching time of 10s (Fig.8a). The size of etch pits increases when increasing the etching time and the rectilinear elongated etch patterns (Fig.8b) and rectangular steps (Fig. 8c) suggest that L-Arginine added ZTS crystal has layer growth mechanism. The observed etch pits, attributive to layer growth confirm the two-dimensional nucleation (2D) mechanism with less dislocations [25].



(a)



(b)



(c)

Fig. 8. Etch patterns observed on the (100) face of L-Arginine added ZTS crystal for etching time (a) 10s (b) 30s (c) 60s.

4.8 SHG efficiency studies

The study of NLO conversion efficiency of grown crystals has been carried out in accordance with the classical powder method developed by Kurtz and Perry [26]. A Q-switched Nd:YAG laser beam of wavelength 1064 nm, with an input power of 2.8 mJ and pulse width of 8 ns with a repetition rate of 10 Hz were used. The crystals of ZTS and 1mole% L-Arginine added ZTS were powdered with a uniform particle size and then packed in a micro capillary of uniform bore and exposed to laser

radiation. The output from the sample was monochromated to collect the intensity of 532 nm component, and to eliminate the fundamental wavelength. Second harmonic radiation generated by the randomly oriented micro crystals was focused by a lens and detected by a photo multiplier tube. The generation of second harmonic signal was confirmed by the emission of green light. ZTS, a powdered sample was used as reference material for the present measurement. The measured SHG output signal voltages for powdered samples are given in Table 3.

Table 3. SHG output signal voltage of pure and L-Arginine added ZTS crystals.

| Samples | $I_{2\omega}$ (mV) | SHG efficiency |
|-------------------------|-----------------------|-------------------|
| ZTS | 18 | 1.0 |
| L-Arginine added ZTS | 18.6 | 1.08 |

The SHG conversion efficiency of 1mole% L-Arginine added ZTS is greater than pure ZTS. The enhancement in SHG efficiency of L-Arginine added ZTS is due to the optically active amino group which may get added in the structure and increases its non-centrosymmetry and hence increasing its SHG efficiency.

5. Conclusion

Tristhiourea Zinc(II)sulphate and L-Arginine added Tristhiourea Zinc(II)sulphate compounds were synthesized and optical quality single crystals were grown by slow evaporation solution technique. Single crystal X-ray diffraction confirms that there is no change in structure of ZTS. FT-IR analysis confirms the presence of all functional groups in the synthesized materials. UV-Visible absorption studies show that grown crystals have wide range of transparency in UV and entire visible region and cut-off wavelength is around 268 nm. Thermal analyses show that the grown crystals have thermal stability upto 236 °C. Hardness number (H_v) and work hardening coefficient of the grown crystals have been determined. The perfection and quality of crystals have been identified by using the etching studies. The SHG efficiency increases for L-Arginine added ZTS crystal compared with ZTS. Thus, SHG studies expose that the amino acid L-Arginine added ZTS crystal is a suitable for optoelectronics applications.

Acknowledgements

The authors acknowledge Prof. P. K. Das, Department of Inorganic and Physical Chemistry, Indian Institute of Science, Bangalore, India for laser facilities and Centre for Nano science and technology, Anna University, Chennai, India for thermal studies. Also acknowledge VIT University for powder XRD studies.

References

- [1] N. Prasad, J. Willams, Introduction to Nonlinear optical effect in Molecules and Polymers, John Wiley and Sons, Inc.,(1991).
- [2] S. S. Hussaini, N. R. Dhumane, V. G. Dongre, P. Karmuse, P. Ghughare, M. D. Shirsat, Optoelectron. Adv. Mater.- Rapid Commun. **2**, 108 (2008).
- [3] R. Mohan Kumar, D. Rajan Babu, D. Jayaraman, R. Jayavel, K. Kitamura, J. Cryst. Growth. **275**, 935 (2005).
- [4] K. Meera, R. Muralidharan, R. Dhanasekaran, Manyum Prapun, P. Ramasamy, J. Cryst. Growth. **263**, 510 (2004).
- [5] G. D. Andreetti, L. Cavalca, A. Musatti, Acta Crystallogr. Sect. B **24**, 683 (1968).
- [6] S. Moitra, T. Kar, Optical Materials. **30**, 508 (2007).
- [7] S. Mukerji, T. Kar, Mater. Res. Bull. **33**, 619 (1998).
- [8] S. S. Hussaini, N. R. Dhumane, V. G. Dongre, M. D. Shirsat, J. Materials Science-Poland **27**, 365 (2009).
- [9] S. Gao, W. Chen, G. Wang, J. Chen, J. Cryst. Growth. **297**, 361 (2006).
- [10] P. Joseph Ginson, J. Philip, K. Rajarajan, S. A. Rajasekar, A. Joseph Arul Pragasam, K. Thamizharasan, S. M. Ravi Kumar, P. Sagayaraj, J. Cryst. Growth. **296**, 51 (2006).
- [11] P. M. Ushasree, R. Muralidharan, R. Jayavel, P. Ramasamy, J. Cryst. Growth, **210**, 741 (2000).
- [12] S. Dhanuskodi, K. Vasanth, P. A. Angeli Mary, Spectrochim. Acta Part A **66**, 637 (2007).
- [13] S. S. Gupte, C. P. Desai, Cryst. Res. Technol. **34**, 1329 (1999).
- [14] J. Ramajothi, S. Dhanuskodi, K. Nagarajan, Cryst. Res. Technol. **39**, 414 (2004).
- [15] M. Oussaid, P. Becker, M. Kemiche, C. Carabatos-Nedelec, Phys. Stat. Sol.(b) **207**, 103 (1998).
- [16] P. M. Ushasree, R. Jayavel, C. Subramanian, P. Ramasamy, J. Cryst. Growth. **197**, 216 (1999).
- [17] P. M. Ushasree, R. Jayavel, P. Ramasamy, Mater. Chem. Phys. **61**, 270 (1999).
- [18] G. Arunmozhi, M. de Gomes, S. Ganesamoorthy, Cryst. Res. Technol. **39**, 408 (2004).
- [19] P. A. Angeli Mary, S. Dhanuskodi, Cryst. Res. Technol. **36**, 1231 (2001).
- [20] N. R. Dhumane, S. S. Hussaini, V. V. Nawarkhele, M. D. Shirsat, Cryst. Res. Technol. **41**, 897 (2006).
- [21] K. Kanagasabapathy, R. Rajasekaran, Optoelectron. Adv. Mater. - Rapid Commun. **6**(1-2), 218 (2012).
- [22] P. M. Ushasree, R. Jayavel, P. Ramasamy, Mater. Sci. Eng. B **65**, 153 (1999).
- [23] R. Bairava Ganesh, V. Kannan, R. Sathyalakshmi, P. Ramasamy, Mater. Lett. **61**, 706 (2007).
- [24] E. M. Onitsch, Mikroskopie, **2**, 131 (1947).
- [25] L. J. Farrugia, J. Appl. Crystallogr. **32**, 837 (1999).
- [26] S. K. Kurtz, T. T. Perry, J. Appl. Phys. **39**(8), 3798 (1968).